Differential stability of β-catenin along the animal-vegetal axis of the sea urchin embryo mediated by dishevelled

Heather E. Weitzel[1], Michele R. Illies[1], Christine A. Byrum[2], Ronghui Xu[2], Athula H. Wikramanayake[2] and Charles A. Ettensohn[1,*]

[1]Department of Biological Sciences, Carnegie Mellon University, 4400 Fifth Avenue, Pittsburgh, PA 15213, USA
[2]Department of Zoology, University of Hawaii at Manoa, 2538 McCarthy Mall, Honolulu, HI 96822, USA
*Author for correspondence (e-mail: ettensohn@andrew.cmu.edu)

Accepted 2 March 2003

Development 131, 2947-2956
Published by The Company of Biologists 2004
doi:10.1242/dev.01152

Summary

β-Catenin has a central role in the early axial patterning of metazoan embryos. In the sea urchin, β-catenin accumulates in the nuclei of vegetal blastomeres and controls endomesoderm specification. Here, we use in-vivo measurements of the half-life of fluorescently tagged β-catenin in specific blastomeres to demonstrate a gradient in β-catenin stability along the animal-vegetal axis during early cleavage. This gradient is dependent on GSK3β-mediated phosphorylation of β-catenin. Calculations show that the difference in β-catenin half-life at the animal and vegetal poles of the early embryo is sufficient to produce a difference of more than 100-fold in levels of the protein in less than 2 hours. We show that dishevelled (Dsh), a key signaling protein, is required for the stabilization of β-catenin in vegetal cells and provide evidence that Dsh undergoes a local activation in the vegetal region of the embryo. Finally, we report that GFP-tagged Dsh is targeted specifically to the vegetal cortex of the fertilized egg. During cleavage, Dsh-GFP is partitioned predominantly into vegetal blastomeres. An extensive mutational analysis of Dsh identifies several regions of the protein that are required for vegetal cortical targeting, including a phospholipid-binding motif near the N-terminus.

Key words: β-Catenin, Dishevelled, GSK3β, Sea urchin embryo, Early patterning

Introduction

β-Catenin plays multiple, important roles in patterning animal embryos. This protein is an essential component of the highly conserved, canonical Wnt signaling pathway, which has been studied intensively in embryonic and cancer cells (reviewed by Huelsken and Behrens, 2002; Moon et al., 2002). According to the current view of the canonical pathway, Wnt signaling leads to the stabilization of cytosolic β-catenin. In the absence of a Wnt signal, β-catenin is phosphorylated at several N-terminal serine and threonine residues, first by a priming kinase, casein kinase I (CKI), and then by glycogen synthase kinase-3-β (GSK3β). Phosphorylation by GSK3β targets β-catenin for ubiquitination and proteasome-mediated degradation. Phosphorylation of β-catenin occurs in a multiprotein complex that includes GSK3β, Axin (a scaffolding protein), the tumor suppressor gene product adenomatous polyposis coli protein (APC), and several other proteins. Binding of secreted Wnt ligands to frizzled receptors inhibits the degradation of β-catenin via the activation (possibly by phosphorylation) of dishevelled (Dsh). Activated Dsh inhibits GSK3β by a mechanism that remains unclear but that might involve recruitment of GBP/FRAT1 to the degradation complex (Ferkey and Kimelman, 2002; Hino et al., 2003). Increased cytoplasmic pools of β-catenin are thought to lead to accumulation of the protein in the nucleus, where β-catenin interacts with LEF/TCF transcription factors and activates the transcription of Wnt-responsive genes. Although it has sometimes been argued that signaling may not be regulated by total or nuclear levels of β-catenin (e.g. Chan and Struhl, 2002), a large body of evidence from many experimental systems has shown a correlation between levels of nuclear β-catenin and signaling (see discussion in Guger and Gumbiner, 2000; Henderson and Fagotto, 2002; Tolwinski et al., 2003).

Recent studies have demonstrated that β-catenin has a highly conserved function in patterning early metazoan embryos. In all deuterostome embryos that have been closely examined in this regard, including those of amphibians, fish, chicks, ascidians and sea urchins, β-catenin becomes localized to cell nuclei preferentially at one pole of the cleavage-stage embryo (Schneider et al., 1996; Larabell et al., 1997; Rowning et al., 1997; Logan et al., 1999; Roeser et al., 1999; Imai et al., 2000). In these various organisms, nuclear activity of β-catenin, through its interaction with LEF/TCF proteins, is required for early axis specification and the establishment of critical signaling centers in the early embryo (Heasman et al., 1994; Kelly et al., 1995; Wylie et al., 1996; Pelegri and Maischein, 1998; Imai et al., 2000; Kelly et al., 2000). Recent studies with cnidarian embryos suggest that this mechanism of axis specification might be very ancient; i.e. its origins may pre-date the divergence of radially and bilaterally symmetrical metazoans (Wikramanayake et al., 2003).

In the sea urchin, β-catenin is required for the formation of endoderm and mesoderm. Overexpression of proteins that interfere with nuclear localization and/or function of β-catenin, including cadherins, GSK3β and a dominant negative form of

TCF/LEF, lead to the development of 'dauerblastula' embryos, which lack mesenchyme cells and gut (Emily-Fenouil et al., 1998; Wikramanayake et al., 1998; Logan et al., 1999; Vonica et al., 2000). β-Catenin appears to have multiple functions in endomesoderm specification. In the large micromere-primary mesenchyme cell (PMC) lineage, β-catenin is an essential activator of a network of early zygotic transcription factors, including Pmar1, Ets1, Alx1 and T-brain, that regulate the powerful signaling properties and later morphogenesis of these cells (Kurokawa et al., 1999; Fuchikami et al., 2002; Oliveri et al., 2002, 2003; Sweet et al., 2002; Ettensohn et al., 2003). In the macromeres, β-catenin is required for the activation of genes involved in endoderm and non-skeletogenic mesoderm specification, including those that render the cells responsive to micromere-derived signals (McClay et al., 2000; Davidson et al., 2002). β-Catenin also plays an indirect role in ectoderm specification, through its influence on vegetally derived signals that pattern the overlying ectoderm (Wikramanayake et al., 1998).

Although the regulation of nuclear localization and function of β-catenin is a critical feature of early metazoan development, the underlying mechanisms are not well understood. It has been proposed that the differential nuclear accumulation of β-catenin is a consequence of regulated proteolytic degradation along the embryo axis. This hypothesis is based on experiments demonstrating that overexpression of proteins predicted to interfere with or enhance β-catenin degradation lead to corresponding changes in nuclear localization and axis specification (see reviews by Moon and Kimelman, 1998; Sokol, 1999). Although overexpression studies point strongly to differential degradation, there has been no direct demonstration that the stability of β-catenin varies along an early embryo axis. One study compared the half-life of β-catenin on the dorsal and vegetal sides of the cleavage-stage *Xenopus* embryo using biochemical methods but reported that β-catenin was highly and equally stable ($t_{1/2}$=3.6-3.8 hours) on both sides of the embryo (Guger and Gumbiner, 2000). Mechanisms other than regulated proteolysis have also been put forward to account for changes in levels of nuclear β-catenin, including regulated nuclear import/export and interactions with cytoplasmic and nuclear anchoring proteins (Henderson and Fagotto, 2002). One recent study, for example, has argued that Wnt signaling increases levels of nuclear β-catenin not by regulating GSK3β-mediated degradation, but by triggering the degradation of a cytoplasmic anchoring protein (Tolwinski et al., 2003).

In the present study, we have exploited the optical transparency of the sea urchin embryo to measure the half-life of β-catenin in specific cell lineages in vivo. We report a gradient in β-catenin stability along the animal-vegetal (A-V) axis during cleavage and show that degradation of β-catenin in animal blastomeres is dependent on GSK3β-mediated phosphorylation of the protein. We find that overexpression of a dominant negative form of Dsh blocks nuclear accumulation of β-catenin in vegetal cells and suppresses mesoderm and endoderm formation. Finally, we report that a GFP-tagged form of Dsh shows a striking, specific localization to the vegetal cortex of the fertilized egg and early vegetal blastomeres, where we propose it is locally activated and subsequently functions to stabilize β-catenin. Through a detailed mutational analysis of Dsh, we have identified several regions that are required for vegetal targeting, including a short phospholipid-binding motif within the DIX domain of the protein.

Materials and methods

Animals

Adult *Lytechinus variegatus* were obtained from the Duke University Marine Laboratory (Beaufort, NC) and Carolina Biological Supply (Burlington, NC). Spawning was induced by intracoelomic injection of 0.5 M KCl. For most experiments, embryos were cultured at 23°C in temperature-controlled waterbaths.

Cloning of LvDsh, LvAxin and LvGSK3β

A 600-bp fragment of LvDsh was cloned by RT-PCR from mesenchyme blastula-stage cDNA using degenerate primers. 5′- and 3′-RACE were used to isolate clones containing the remainder of the coding sequence and the 5′ and 3′ untranslated regions. A single cDNA clone encoding a fragment of Axin from *Strongylocentrotus purpuratus* was identified in an EST sequencing project (Zhu et al., 2001). PCR primers designed from this sequence were used to amplify a fragment of LvAxin from unfertilized egg-stage cDNA. 5′- and 3′-RACE were used to isolate clones containing the remainder of the sequence. LvGSK3β was cloned by RT-PCR using the published sequence of GSK3β from *Paracentrotus lividus* and primer sequences described by Emily-Fenouil et al. (1998). Sequences of LvDsh, LvAxin, and LvGSK3β have been deposited in GenBank (Accession numbers AY624074, AY624075 and AY624076, respectively).

RNA injection and immunostaining

For mRNA injections, cDNAs were subcloned into pCS2+MT or pCS2+GFP vectors. Injections of in-vitro transcribed, capped mRNAs were carried out as described (Sweet et al., 2002). Immunostaining with anti-β-catenin antibody was performed following the protocol of Logan et al. (1999), except that embryos were fixed for 4 hours. Point mutations in LvDsh were introduced using the Quick-Change Site-Directed Mutagenesis Kit (Stratagene) and deletions were generated by PCR.

4-D confocal laser scanning microscopy

Four-dimensional microscopy was carried out using a Bio-Rad MRC-600 laser-scanning microscope equipped with 40× and 60× water immersion objectives. Z-stacks (20-40 images/stack) of 256×256 pixel images were collected every 2 minutes with a step size of 4 μm, using Kalman filtering and the Fast1 scan rate. Acquisition of the stacks was automated using the SOM program (dlapse) accessible through the CoMos software package (Bio-Rad). A two-dimensional projection (maximum-intensity method) was generated from each z-stack and transferred to a Macintosh G4 computer. NIH Image was used to generate time-lapse sequences of the two-dimensional projections. Representative (non-time-lapse) images of embryos expressing various GFP-tagged proteins were obtained by confocal microscopy as described above, except that z-stacks were collected at a slow scan rate with a step size of 1-2 μm and an image size of 512×512 pixels.

Measurements of protein half-life in vivo

To calculate the half-life of GFP-tagged proteins, fertilized eggs were injected with mRNA encoding the protein of interest and allowed to develop for a period of time sufficient for accumulating levels of the GFP-tagged product detectable by confocal microscopy. At various times, the translational inhibitor emetine was added to the cultures (final concentration=100 μM) and the embryos were cultured continuously in the presence of the inhibitor. After 30 minutes, when emetine was maximally effective, time-lapse sequences were collected as described above. Each sequence encompassed 45-60

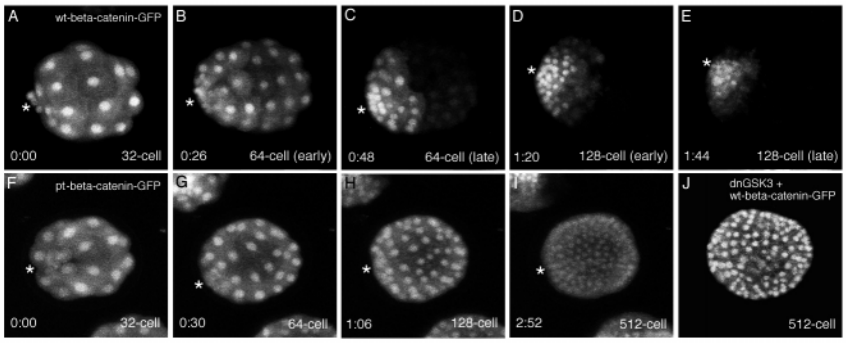

Fig. 1. Four-dimensional confocal analysis of Xl-β-catenin-GFP expression. (A-E) Frames from a time-lapse sequence following injection of Xl-wt-β-catenin-GFP mRNA at the 1-cell stage. Times after the start of recording (hours:minutes) are shown in the bottom left corner of each panel and cell number is shown in the bottom right corner. GFP-tagged β-catenin was initially localized in the nuclei, cytoplasm and junctional complexes of all blastomeres (A). GFP-tagged β-catenin disappeared from the animal region of the embryo over a period of approximately two cell cycles (B-E). GFP-tagged β-catenin eventually became restricted to a small territory of cells surrounding the vegetal pole (asterisk). (F-I) Frames from a time-lapse sequence following injection of Xl-pt-β-catenin-GFP at the 1-cell stage. Mutation of residues phosphorylated by GSK3β and a priming kinase at the N-terminus of β-catenin blocked the disappearance of GFP-tagged protein from animal blastomeres. The vegetal pole is marked by an asterisk. (J) Co-injection of mRNAs encoding Xl-wt-β-catenin-GFP and a kinase-dead, dominant negative form of GSK3β (Xl-dnGSK3β) at the 1-cell stage. Expression of dnGSK3β stabilized GFP-tagged β-catenin in animal blastomeres.

minutes of real time. To ensure that the intensity of all fluorescence images was below saturation, the CoMos software was used to examine histograms of pixel intensities in the 8-bit images and settings on the MRC-600 were adjusted such that the brightest pixel in the raw images in each sequence had an intensity value of <256. From the maximal-intensity projections of each z-stack, NIH Image was used to measure the mean pixel intensity within selected regions of each frame. Average pixel intensities were measured in specific cell lineages by hand-selecting the cells using a free-form tool. These values represented average pixel intensities over the entire cellular region, i.e. including both nuclear and cytoplasmic pools of protein. Initial average pixel values (30 minutes after addition of emetine) were set to 1 and the natural log (ln) of average pixel intensity was plotted versus time using Microsoft Excel. These plots showed a linear decrease in pixel intensity over time, as expected for an exponential decay (Fig. 2D). A trend line was added to each curve and used to determine the R^2 value and the equation of the line ($y=mx+b$). The slope (m) was used in the equation $t_{1/2}=0.693/m$ to calculate the half-life ($t_{1/2}$) of the fluorescence in each cell lineage.

^{35}S-methionine experiments

Cleavage-stage embryos were incubated in emetine for 25 minutes and 20 μCi/ml ^{35}S-methionine was then added to the medium for 15 minutes. After TCA precipitation, incorporation of the radioactive label was measured with a scintillation counter. Levels of incorporation were plotted relative to sibling embryos not exposed to emetine.

Results

Dynamics of β-catenin turnover in vivo and regulation by GSK3β

Using the optically transparent embryos of *Lytechinus variegatus*, we expressed GFP-tagged *Xenopus* β-catenin (Xl-wt-β-catenin-GFP) and followed the dynamics of protein expression using 4-D confocal laser-scanning microscopy (Fig. 1). Microinjection of in-vitro transcribed, capped mRNA encoding Xl-wt-β-catenin-GFP resulted in detectable protein expression by the 2-cell stage. Initially, the protein was expressed at similar levels in all blastomeres (Fig. 1A); in the cytoplasm and nucleus, and in association with cell membranes. Later in cleavage, levels of GFP fluorescence (both cytoplasmic and nuclear) in animal blastomeres declined dramatically (Fig. 1B-E). Over 1-2 cell cycles, nuclear Xl-wt-β-catenin-GFP became restricted to a region at the vegetal pole of the embryo that included the micromere territory and the vegetal-most portion of the macromere territory. This restricted pattern of Xl-wt-β-catenin-GFP nuclear localization closely matched the normal vegetal nuclear accumulation of β-catenin in *L. variegatus* embryos, visualized using an antibody against the endogenous protein (Logan et al., 1999).

The precise stage at which the loss of β-catenin-GFP in animal blastomeres was first detectable, and the final boundary of the vegetal domain of nuclear β-catenin-GFP, varied with the amount of mRNA injected. At relatively low doses, clearing could be detected as early as the 16-cell stage, and nuclear β-catenin-GFP became restricted to the micromere territory and small numbers of veg2-derived cells. At higher doses, loss of fluorescence in the animal blastomeres was delayed until the 64-128-cell stages and larger numbers of cells of the veg2 territory retained nuclear β-catenin. Overexpression of Xl-wt-β-catenin-GFP produced no apparent phenotype, despite the transient nuclear localization of the protein in animal blastomeres.

The loss of β-catenin in animal blastomeres was dependent on GSK3β, a serine-threonine kinase that phosphorylates β-catenin on several N-terminal residues and targets the protein for ubiquitination and degradation. We expressed a GFP-tagged form of *Xenopus* β-catenin (Xl-pt-β-catenin-GFP) in which four N-terminal serine and threonine residues were converted to alanines. Three of these residues are phosphorylated by GSK3β and one by a priming kinase, casein kinase 1 (Yost et al., 1996; Liu et al., 2002). This variant of β-catenin shows increased stability in biochemical assays and in vivo (Yost et al., 1996; Guger and Gumbiner, 2000). Overexpression of Xl-pt-β-catenin-GFP resulted in persistent nuclear localization of the protein in all blastomeres throughout cleavage and blastula stages (Fig. 1F-I). Similarly, coexpression of Xl-wt-β-catenin-GFP and a kinase-dead, dominant negative form of *Xenopus* GSK3β (Xl-dn-GSK3β) prevented the loss of β-catenin from animal blastomeres (Fig. 1J). Overexpression of Xl-pt-β-catenin-GFP or Xl-dn-GSK3β resulted in a vegetalized phenotype, as previously reported (Emily-Fenouil et al., 1998; Wikramanayake et al., 1998). These studies indicated that the restriction of nuclear β-catenin-GFP to the vegetal region is dependent on GSK3β-mediated degradation of the protein in animal blastomeres.

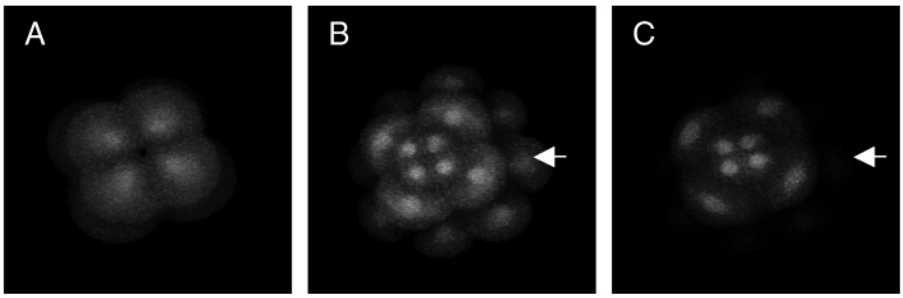

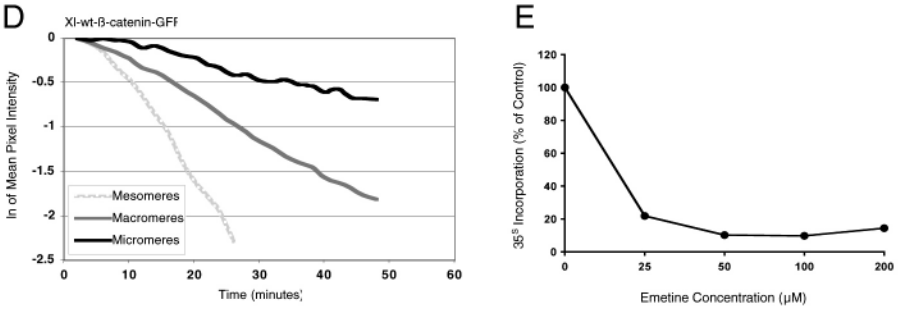

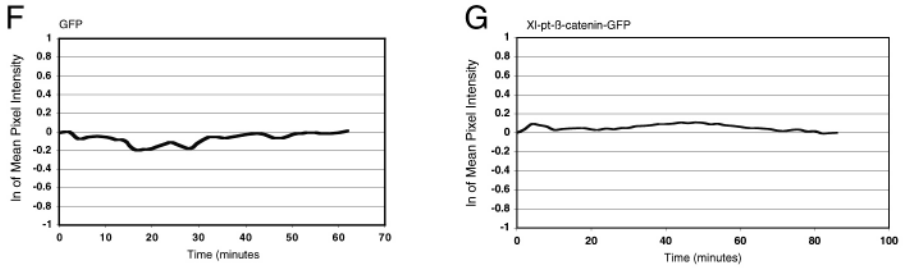

H

Cell Type	Avg. Half-life (hr)	Std. Dev.	n
Mesomeres	0.24	0.12	11
Macromeres	0.59	0.36	8
Veg1	0.74	0.07	3
Veg2	0.93	0.21	3
Micromeres	1.60	1.02	11

Avg. Micromere:Mesomere Half-Life Ratio	Std. Dev.	n
8.25	3.0	10

Fig. 2. In-vivo measurements of β-catenin-GFP half-life. (A-C) Measurement of β-catenin-GFP half-life at the 16-cell stage. Confocal projections (vegetal views) of an embryo expressing Xl-wt-β-catenin-GFP. Emetine was added immediately after the third cleavage division (A), and after 30 minutes in the presence of the inhibitor the embryo had completed fourth cleavage (B). Loss of β-catenin-GFP was apparent in animal blastomeres during the ensuing 30 minutes (arrows, B,C). (D) Representative data from a single embryo, showing decay of GFP fluorescence in specific cell lineages as measured by 4-D confocal microscopy. 0 on the *x*-axis corresponds to 30 minutes after addition of emetine. (E) Control experiment measuring ^{35}S-methionine incorporation after 25 minutes' exposure to varying concentrations of emetine. 100 μM emetine blocked ~90% of new protein synthesis. (F) Control for GFP photobleaching. Fertilized eggs were injected with mRNA encoding GFP and allowed to develop to the 8-cell stage. Embryos were treated with 100 μM emetine for 30 minutes and then imaged with 4-D confocal microscopy under conditions identical to those shown in Fig. 1. These representative data from a single embryo show that GFP fluorescence (mean fluorescent pixel intensity measured over the entire embryo) remained constant over the period of the experiment. 0 on the *x*-axis corresponds to 30 minutes after addition of emetine. (G) Decay in GFP fluorescence is dependent on β-catenin phosphorylation. Fertilized eggs were injected with Xl-pt-β-catenin-GFP mRNA. At the 8-cell stage, embryos were treated with 100 μM emetine for 30 minutes and then imaged with 4-D confocal microscopy under conditions identical to those shown in Fig. 1. These representative data from a single embryo show that GFP fluorescence (mean fluorescent pixel intensity measured over the entire embryo) remained constant over the period of the experiment. (H) Summary of Xl-wt-β-catenin-GFP half-life measurements. Half-life was measured in different cell lineages of cleavage stage embryos and data were pooled from 8-, 16- and 64-cell stage embryos. On average, within any individual embryo, the half-life of β-catenin-GFP in the vegetal-most blastomeres (the micromere territory) was more than 8-fold greater than in the animal blastomeres (the mesomere territory).

Measurements of b-catenin half-life in vivo

To measure the half-life of β-catenin in specific cell lineages, we injected mRNA encoding Xl-wt-β-catenin-GFP into fertilized eggs, allowed the protein to accumulate to levels detectable by confocal microscopy, then blocked further protein translation with emetine. Control experiments showed that 100 μM emetine inhibited >90% of new protein synthesis within 20 minutes (Fig. 2E). Levels of fluorescence were quantified over the subsequent 45-60 minutes and the rate of fluorescence decay was used to calculate the half-life of the protein in different blastomeres (Fig. 2). Additional control experiments showed that fluorescence decay was dependent on GSK3β-mediated phosphorylation of β-catenin and that photobleaching of GFP was negligible over the time course of our experiments (Fig. 2F-G).

These measurements provided direct evidence of a gradient in β-catenin stability along the A-V axis during early cleavage. The average half-life of β-catenin-GFP in the mesomere, macromere and micromere territories was 0.24, 0.59 and 1.60 hours, respectively (Fig. 2H). In our emetine experiments, we detected differential degradation of β-catenin as early as the 8-cell stage (approximately 2 hours postfertilization), the first stage at which cleavage divisions separated animal from vegetal blastomeres. We also made half-life measurements at

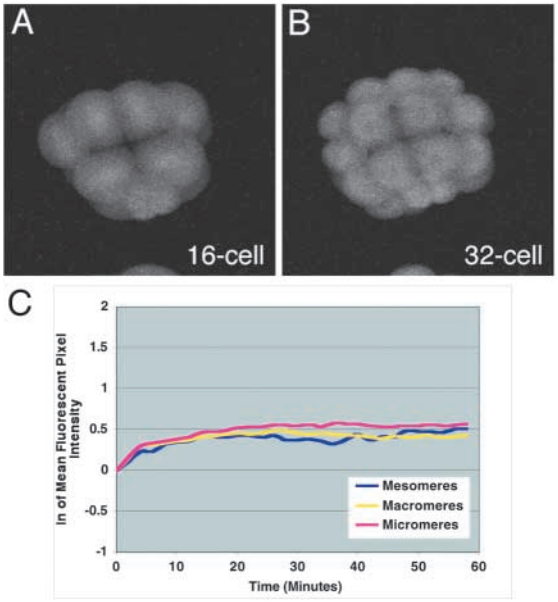

Fig. 3. GSK3β-GFP is uniformly stable along the animal-vegetal (A-V) axis during cleavage. (A,B) Two frames from a time-lapse 4-D confocal sequence following injection of Lv-GSK3β-GFP mRNA at the 1-cell stage. The protein is found in all blastomeres during early cleavage and does not appear to be enriched in a specific subcellular compartment. (C) Quantitation of Lv-GSK3β-GFP turnover following emetine treatment at the 16-cell stage. The protein is equally and highly stable in mesomere, macromere and micromere territories.

the 16- and 64-cell stages and consistently observed a gradient in β-catenin stability at these stages. We found no striking increase or decrease in β-catenin stability within any single cell lineage between the 8- and 64-cell stages, and therefore data from these various cleavage stages were pooled in the table shown in Fig. 2H.

Potential regulators of β-catenin degradation: GSK3β and dishevelled

The differential stability of β-catenin along the A-V axis suggested that positive or negative regulators of degradation might be localized (or activated) in the animal or vegetal regions, respectively. Localized degradation of GSK3β has been proposed as a mechanism for regulating nuclear accumulation of β-catenin in the early *Xenopus* embryo (Dominguez and Green, 2000). We cloned GSK3β from *L. variegatus* (GenBank Accession number AY624076) and expressed a GFP-tagged form, but half-life measurements showed that the protein was highly and equally stable in all blastomeres (Fig. 3). Dorsal translocation of dishevelled (Dsh) following fertilization has also been proposed to play a role in *Xenopus* (Miller et al., 1999). We cloned Dsh from *L. variegatus* (GenBank Accession number AY624074) and found that LvDsh mRNA was ubiquitously expressed in eggs and early embryos (data not shown). We expressed a GFP-tagged form of LvDsh (Lv-wt-Dsh-GFP) and observed a striking, vegetal cortical localization (VCL) of the protein (Fig. 4). At the light microscope level, Lv-wt-Dsh-GFP accumulated in punctate structures associated with the cortical cytoplasm in the vegetal region (Fig. 4F). We also observed punctate localization to the perinuclear region of all cells, including animal blastomeres. In some embryos injected with high concentrations of mRNA, VCL could be detected even before first cleavage (Fig. 4A). Continuous observation of such embryos showed that the first and second cleavage planes bisected the domain of Lv-wt-Dsh-GFP localization. The third cleavage unambiguously identified this region as the vegetal pole. At the 16-cell stage, the VCL domain was inherited by the micromeres and, to a lesser extent, the macromeres. The VCL domain became more difficult to detect at later stages, but could be identified in some embryos as late as the 32-cell stage.

Mutational analysis of LvDsh

Dsh is a multi-domain protein that interacts with many partners (Penton et al., 2002, Wharton, 2003). We generated deletions and point mutations in LvDsh to determine which domains were required for VCL (Figs 5, 6). Although we did not quantify expression levels of the various protein constructs by immunoblotting, all were expressed at levels that were readily detectable by fluorescence microscopy. It was apparent that vegetal targeting did not correlate with relative levels of expression based on GFP fluorescence, i.e. of some constructs that yielded very bright fluorescence, some showed targeting while others did not, and the same was true of constructs that showed faint fluorescence. In addition, all constructs were injected over at least a 10-fold range of concentration and we

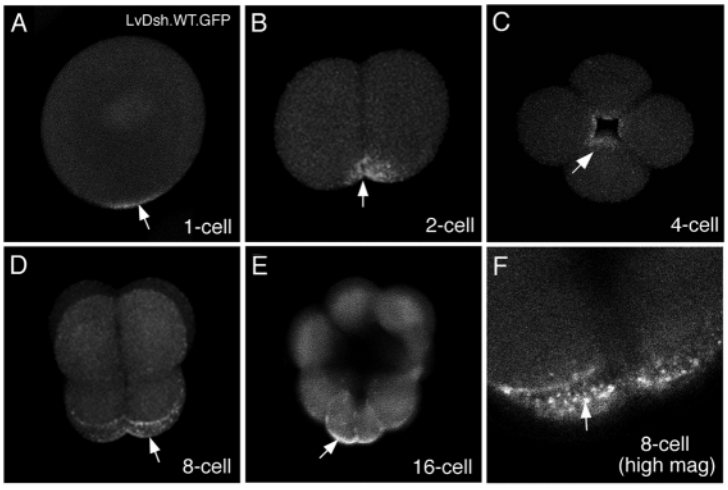

Fig. 4. Vegetal, cortical targeting of GFP-tagged LvDsh. (A) Fertilized egg. LvDsh-GFP (wild-type) targeted to one pole of the fertilized egg even before first cleavage (arrow). (B) Two-cell stage. The first cleavage plane bisected the zone of cortically localized LvDsh-GFP (arrow). (C) 4-cell stage. (D) 8-cell stage. LvDsh-GFP was concentrated in the vegetal cortex of the four vegetal blastomeres (arrow), which were slightly smaller than the four animal blastomeres. (E) 16-cell stage. The region of cortically localized LvDsh-GFP was inherited by the micromeres (arrow) and, to a lesser extent, the overlying macromeres. (F) High magnification view of the vegetal cortical region of vegetal blastomeres at the 8-cell stage, showing the punctate nature of GFP fluorescence (arrow). All panels show different embryos and all show lateral views except (C), which is viewed along the A-V axis.

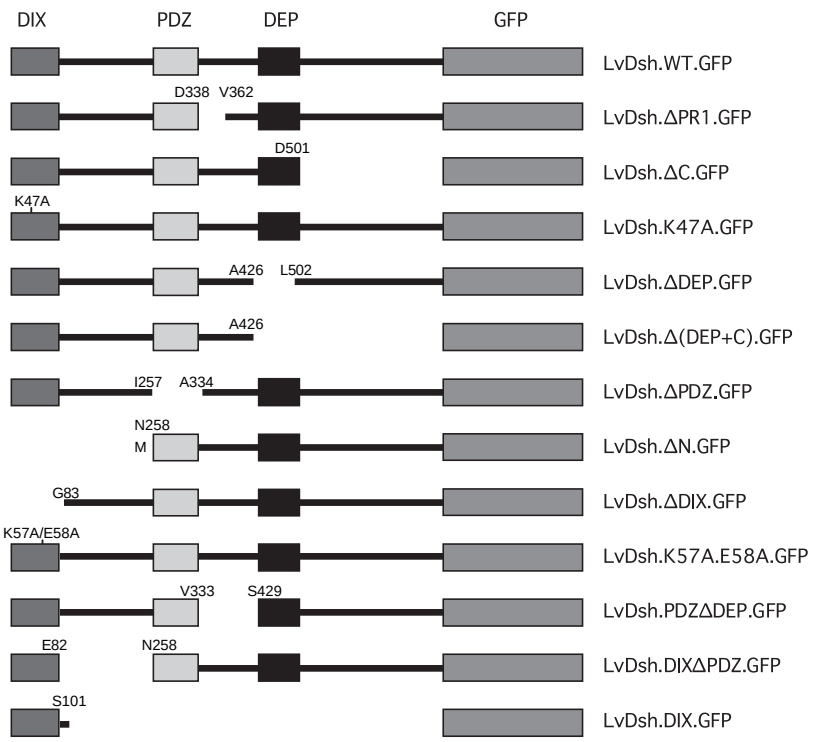

	VCL
LvDsh.WT.GFP	+
LvDsh.ΔPR1.GFP	+
LvDsh.ΔC.GFP	+
LvDsh.K47A.GFP	+
LvDsh.ΔDEP.GFP	+/-
LvDsh.Δ(DEP+C).GFP	+/-
LvDsh.ΔPDZ.GFP	+/-
LvDsh.ΔN.GFP	-
LvDsh.ΔDIX.GFP	-
LvDsh.K57A.E58A.GFP	-
LvDsh.PDZΔDEP.GFP	-
LvDsh.DIXΔPDZ.GFP	-
LvDsh.DIX.GFP	-

Fig. 5. Analysis of LvDsh domains required for vegetal, cortical localization (VCL). Mutant constructs and their designations are indicated. '+' indicates that VCL was evident in essentially all embryos oriented favorably; '+/–' indicates that some favorably oriented embryos, but not all, exhibited VCL. In addition, in those embryos in which VCL was apparent, the crescent of Dsh-GFP was generally less pronounced than observed following injection of mRNA encoding wild-type LvDsh-GFP. '–' indicates that essentially no embryos with unambiguous VCL could be identified.

did not detect changes in the distribution of GFP-tagged proteins over this range.

A putative SH3-binding motif (see Penton et al., 2002) and the C-terminal region of LvDsh were completely dispensible for VCL (Fig. 5; LvDsh.ΔPR1.GFP and LvDsh.ΔC.GFP, respectively). Deletion of the DEP or PDZ domains [LvDsh.ΔDEP.GFP and LvDsh.ΔPDZ.GFP, respectively; see also LvDsh.Δ(DEP+C).GFP)] only partially suppressed VCL. Deletion of the entire N-terminal region (LvDsh.ΔN.GFP), however, or the DIX domain (LvDshΔDIX.GFP) alone, completely abolished targeting.

Motifs within the DIX domain have been identified that regulate binding to actin and vesicles in cultured mammalian cells. Point mutations in the actin-binding motif (K58A) and vesicle (phospholipid)-binding motif (K68A/E69A) have been shown to abolish the corresponding binding activities without compromising the structural integrity of the DIX domain (Capelluto et al., 2002). These two motifs are well conserved within the DIX domain of LvDsh. A point mutation in the actin-binding domain of LvDsh (LvDsh.K47A.GFP) that corresponded to the K58A mutation described by Capelluto et al. (2002) did not affect VCL, but the corresponding double mutation in the phospholipid-binding domain (LvDsh.K57A/E58A.GFP) completely abolished targeting (Fig. 5; Fig. 6E). Two other regions were identified that were required for targeting: a region between the DIX and PDZ domains that includes multiple phosphorylation sites (LvDsh.DIXΔPDZ.GFP) and amino acid sequences other than the proline-rich region that lie between the PDZ and DEP domains (LvDsh.PDZΔDEP.GFP). The smallest portion of the LvDsh protein sufficient for VCL consisted of approximately the N-terminal half of the protein [LvDsh.Δ(DEP+C).GFP].

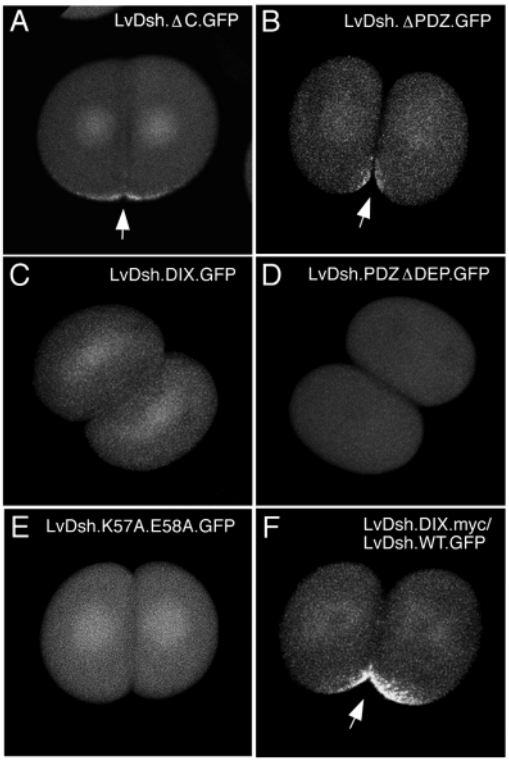

Fig. 6. Selected examples of the localization of GFP-tagged Dsh mutants. Deletion of the C-terminus does not affect VCL (A, arrow) and deletion of the PDZ domain only partially abrogates targeting (B, arrow). VCL is completely blocked by deletion of the DIX domain (C) or the region between the PDZ and DEP domains (D). (E) VCL is also blocked by introducing two point mutations (K57A/E58A) into the phospholipid-binding motif within the DIX domain. (F) Co-injection of LvDsh.WT.GFP and the DIX domain of LvDsh shows that the latter does not exert its dominant negative effect by blocking VCL.

Overexpression of a dominant negative form of LvDsh

To test whether Dsh function was required for the vegetal stabilization of β-catenin, we overexpressed the DIX domain

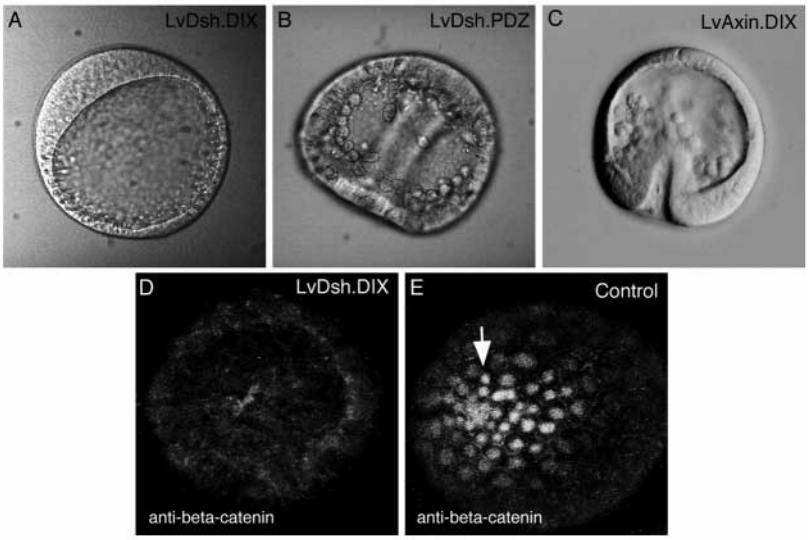

Fig. 7. Dsh function is required for endomesoderm specification and for the accumulation of β-catenin in the nuclei of vegetal blastomeres. (A) Injection of mRNA (1.9 mg/ml) encoding the DIX domain of LvDsh resulted in suppression of endoderm and mesoderm formation and a phenotype indistinguishable from that produced by overexpression of cadherins or GSK3β (Emily-Fenouil et al., 1998; Wikramanayake et al., 1998; Logan et al., 1999). (B,C) Overexpression of the PDZ domain of LvDsh (2.0 mg/ml mRNA) or the DIX domain of LvAxin (3.6 mg/ml mRNA) did not produce apparent phenotypes. Embryos shown in (A-C) are at 20 hours, 20 hours and 18 hours of development, respectively. (D,E) Overexpression of the DIX domain of LvDsh blocked the nuclear accumulation of β-catenin in vegetal blastomeres (arrow, E), as shown by immunostaining using an anti-Lv-β-catenin antibody.

alone. This region of Dsh is required for canonical signaling (Kishida et al., 1999; Rothbacher et al., 2000, Penton et al., 2002) and overexpression of the DIX domain phenocopies Dsh null mutations, indicating that it acts as a dominant negative (Axelrod et al., 1998). We found that overexpression of DIX produced an animalized phenotype that was indistinguishable from the phenotype observed following overexpression of cadherin (Wikramanayake et al., 1998; Logan et al., 1999), i.e. lack of endoderm and reduction or complete absence of mesoderm (Fig. 7A). LvDsh DIX also blocked the accumulation of β-catenin in the nuclei of vegetal blastomeres, as shown by immunostaining with an antibody against endogenous Lv-β-catenin (Fig. 7D,E). At these levels of expression, DIX did not block VCL of Lv-wt-Dsh-GFP (Fig. 6F), indicating that it acted by a different mechanism. By contrast to the striking phenotype resulting from DIX overexpression, overexpression of the PDZ domain of LvDsh had no effect on embryo morphology (Fig. 7B). Axin, another protein that regulates β-catenin degradation, also contains a DIX domain. To determine whether the effects of DIX domain overexpression were specific to LvDsh, we cloned LvAxin (GenBank Accession number AY624075) and overexpressed the LvAxin DIX domain. Injection of LvAxin DIX mRNA at concentrations equal to or higher than LvDsh DIX mRNA produced no apparent phenotype (Fig. 7C).

Discussion

Our in-vivo measurements provide the first direct demonstration of differential stability of β-catenin along an axis of an early metazoan embryo. We have found a gradient in β-catenin half-life along the A-V axis of the sea urchin embryo at early cleavage stages. On average, the protein is approximately 8 times more stable in the most vegetal cells, the micromeres, than in animal blastomeres. This difference in protein stability in the micromere and mesomere territories is sufficient to produce a >100-fold difference in protein levels in 2 hours, approximately the time required for the fertilized egg to reach the 8-cell stage. Averaged over all cell lineages, our estimates of β-catenin half-life in the early sea urchin embryo are consistent with those previously reported based on bulk biochemical analyses of whole *Xenopus* embryos (Yost et al., 1996) (see also Guger and Gumbiner, 2000), whole *Drosophila* embryos (Pai et al., 1997) and tissue culture cells (Byers et al., 1996).

Several observations indicate that the turnover of *Xenopus* wild-type β-catenin-GFP mimics that of the endogenous sea urchin protein. Most significantly, the pattern of nuclear accumulation of Xl-wt-β-catenin-GFP we observed (Fig. 1) closely matches the pattern of nuclear localization of endogenous, sea urchin β-catenin detected by immunostaining (Logan et al., 1999). In addition, several studies have shown that homologous Wnt pathway proteins from vertebrates and sea urchins are functionally interchangeable and therefore likely to be regulated in similar ways. For example, *Xenopus* and sea urchin forms of cadherins, GSK3β and LEF/TCF have been tested in overexpression studies, and in each case the homologs have similar effects (Emily-Fenouil et al., 1998; Wikramanayake et al., 1998: Logan et al., 1999; Vonica et al., 2000). In cnidarians, much more distant relatives of vertebrates than sea urchins, the *Xenopus* wild-type β-catenin construct used in this study has been compared to a GFP-tagged form of the endogenous protein and the two have identical dynamics (Wikramanayake et al., 2003).

The findings reported here point to differential proteolysis as the predominant mechanism controlling the polarized nuclear localization of β-catenin during cleavage. Nevertheless, other mechanisms might operate in parallel. β-Catenin mRNA is uniformly distributed in the egg and early embryo (Miller and McClay, 1997), and differential localization of maternal β-catenin mRNA (or localized transcription of the β-catenin gene) is therefore unlikely to be a contributing factor. We cannot rule out differential translation as a contributing mechanism, however, as our mRNA constructs might lack important translational regulatory elements, and the rate of translation of endogenous β-catenin mRNA in animal and vegetal blastomeres has not been measured. If differential translation contributes to the polarized nuclear accumulation of β-catenin, this effect can be overridden by experimental manipulations that alter post-

translational processing of the protein. Thus, endogenous β-catenin can be driven into the nuclei of more animal blastomeres by treating embryos with LiCl, an inhibitor of GSK3β (Logan et al., 1999). Finally, another plausible mechanism is regulated nuclear import and/or export, possibly involving interactions with cytoplasmic or nuclear anchoring proteins (Henderson and Fagotto, 2002; Tolwinski et al., 2003). Our observation that wild-type and hyperstable β-catenin-GFP accumulate in the nuclei of animal blastomeres (the former transiently and the latter persistently) argues strongly against the possibility that animal blastomeres lack factors required for nuclear import or retention. A potential limitation of overexpression studies, however, is that mechanisms that normally regulate nuclear import/export of β-catenin might be overwhelmed. For example, artificially high levels of β-catenin might saturate a cytoplasmic anchoring protein that normally sequesters β-catenin in the cytoplasm of animal blastomeres. Although the differential translation and cytoplasmic sequestration models warrant further study, our findings strongly support the view that differential degradation is a key mechanism regulating the nuclear accumulation of β-catenin during cleavage.

The methods used in the present study do not allow us to determine precisely when the polarity in β-catenin degradation first arises. It is therefore unclear whether differential stability along the A-V axis involves a local activation of degradation in the animal hemisphere, an inhibition of degradation in the vegetal region, or a combination of mechanisms. A difference in β-catenin stability along the A-V axis is clearly established by the 8-cell stage, when animal and vegetal blastomeres are first separated from one another by a horizontal cleavage. The finding that LvDsh-GFP becomes localized at the vegetal pole even prior to first cleavage, however, suggests that the molecular machinery underlying differential degradation is polarized maternally or immediately after fertilization. This observation also indicates that VCL is not dependent on Wnt signals transmitted between blastomeres, consistent with other evidence that cell-cell signaling is not required for vegetal nuclear accumulation of β-catenin in the sea urchin embryo (Logan et al., 1999).

Our finding that endomesoderm specification and nuclear accumulation of β-catenin are suppressed by overexpression of the DIX domain of Dsh, a putative dominant negative form of the protein with respect to canonical Wnt signaling (Axelrod et al., 1998), provides the strongest evidence to date that Dsh normally plays an essential role in early deuterostome embryo polarity. It has been proposed that Dsh plays a role in axis specification in *Xenopus*, based on the finding that Dsh protein becomes concentrated on the dorsal side of the early embryo (Miller et al., 1999) (see below). There are also differences in levels of Dsh phosphorylation along the dorsal-ventral axis (Rothbacher et al., 2000), although their functional significance (and the role of Dsh phosphorylation in general) remains unclear (Wharton, 2003). The function of Dsh in early patterning in *Xenopus* has been controversial because dominant negative approaches have not yet revealed a role for the protein in endogenous axis formation. Dominant negative forms of Dsh that interfere with Wnt-induced secondary axis formation do not suppress the formation of the endogenous dorsal axis (Sokol, 1996). Others have noted possible technical reasons for the failure of these constructs to suppress normal axis formation, however. Levels of expression of dominant negative constructs might be insufficient for competing with maternal pools of protein, particularly if the maternal proteins are already complexed with other molecules (Miller et al., 1999; Rothbacher et al., 2000).

The molecular mechanism of the dominant negative effect of the DIX domain is unknown. This is largely because the mechanism by which Dsh stabilizes β-catenin has not yet been elucidated. It has been proposed that Dsh acts by binding to Axin, via the DIX domains of the two proteins. This interaction might prevent Axin multimerization (Hsu et al., 1999; Kishida et al., 1999; Sakanaka and Williams, 1999) and/or recruit GBP/FRAT-1, an inhibitor of GSK3β, to the degradation complex (Li et al., 1999; Ferkey and Kimelman, 2002; Hino et al., 2003). Dsh also forms multimers via the DIX domain, and this might be important for signaling (Kishida et al., 1999; Rothbacher et al., 2000). These observations are consistent with a number of scenarios by which stray DIX domains might disrupt endogenous Dsh-Dsh, Dsh-Axin and/or Axin-Axin interactions. For example, DIX might compete with endogenous Dsh for binding to Axin but be unable to recruit GBP/FRAT-1 to the degradation complex.

Our observations and those of Miller et al. (Miller et al., 1999) point to striking similarities in Dsh localization in early sea urchin and *Xenopus* embryos. Miller and co-workers reported that in *Xenopus*, endogenous Dsh and a GFP-tagged form of the protein associate with vesicle-like organelles that translocate from the vegetal pole of the fertilized egg to the future dorsal side during cortical rotation. In *L. variegatus*, LvDsh-GFP is associated with granular or vesicular structures in the vegetal region and this association is dependent on a vesicle-binding motif within the DIX domain. The major difference appears to be that Dsh is not redistributed after fertilization in sea urchin eggs, which lack a cortical rotation. Although the mutational analysis of Miller et al. (Miller et al., 1999) was not as detailed as that presented here, both found that association of Dsh-GFP with vesicle-like structures was dependent on the DIX domain, but not the C-terminal region of the protein. One difference between the two studies, however, is that Miller et al. reported that deletion of the DEP or PDZ domains eliminated association with vesicles, while we found that deletion of these domains in LvDsh only partially blocked targeting to the vegetal cortex and association with vesicles in that region. Dsh has been found associated with punctate cytoplasmic structures in a variety of cell types (Axelrod et al., 1998; Itoh et al., 2000), although it is not known whether these structures are the same as the granular or vesicular structures observed in eggs and early embryos.

Significantly, in our experiments, we observed no phenotype associated with overexpression of full length LvDsh, either untagged or GFP-tagged forms, even at mRNA concentrations sufficiently high to compromise embryo viability. Others have shown that animal blastomeres can be converted to more vegetal fates by overexpression of kinase-dead GSK3β (Emily-Fenouil et al., 1998), a mechanism that bypasses Dsh. Moreover, in the present study, we showed that β-catenin can be driven into the nuclei of animal blastomeres by overexpression of kinase-dead GSK3β or mutation of N-terminal phosphorylation sites in β-catenin. These findings show that disruption of β-catenin degradation downstream of Dsh leads to nuclear accumulation of β-catenin in animal

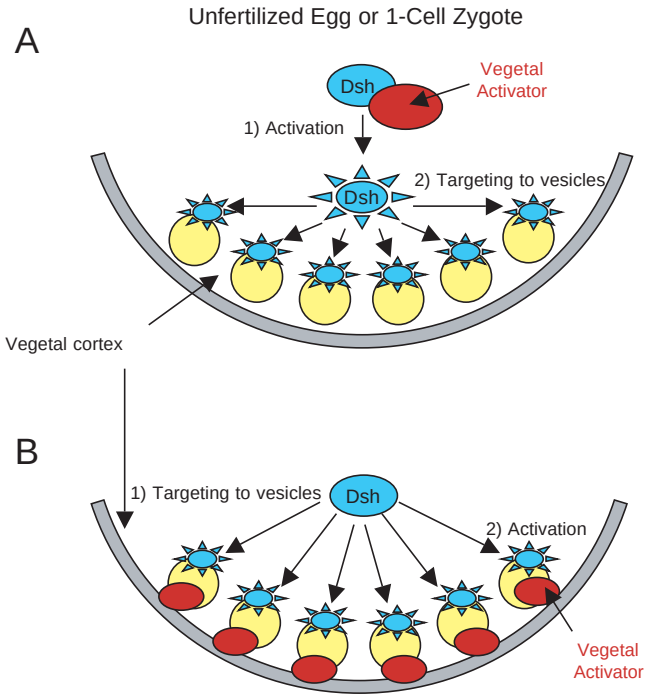

Fig. 8. Models of Dsh activation and targeting in the vegetal region of the unfertilized egg or early embryo. We propose that Dsh is activated specifically in the vegetal region (see Discussion). A putative, vegetally localized activator is shown in red, egg vesicles in yellow, and Dsh in blue. Activated Dsh is shown by a blue star-burst symbol. The activator has not been identified but might be a maternally localized kinase such as Par-1 (Sun et al., 2001). Alternatively, a repressor of Dsh activation might be localized (or activated) in the animal region of the embryo. In Model A, local activation of Dsh triggers targeting to cortical vesicles. This targeting requires a phospholipid-binding motif in the DIX domain of the protein. Although the yellow vesicles are shown localized in the vegetal region of the cell, they might be more widely distributed and Dsh may associate only with those in the vegetal region. In Model B, unactivated Dsh in the vegetal region of the embryo associates with vesicles through the DIX domain, and this association triggers activation of Dsh by the localized activator, which might be associated with vesicles or the vegetal cortex of the egg.

blastomeres and changes in cell fate. Therefore, our finding that overexpression of wild-type LvDsh does not have the same effect strongly suggests that the protein is not active in animal cells. We cannot exclude the possibility that, in our experiments, insufficient levels of LvDsh were expressed in animal blastomeres to produce effects, although GFP-tagging confirmed that the protein was expressed persistently in all cells, including animal blastomeres. An alternative hypothesis, and one that we currently favor, is that Dsh is activated specifically in the vegetal region (Fig. 8). This local activation might involve phosphorylation by a vegetally localized activating kinase or interactions with other vegetal-specific proteins. In light of such a model, the targeting of LvDsh-GFP to the vegetal cortex might be interpreted in one of two ways. First, targeting might be an essential step in Dsh activation. For example, vegetal targeting might bring Dsh into close association with a localized, activating kinase, such as Par-1 (Sun et al., 2001). Alternatively, VCL might be a consequence of the vegetal activation of Dsh. In that event, VCL could serve to concentrate the protein to effective levels in vegetal blastomeres, or it might play no functional role. Further studies will be required to identify the mechanisms and function of the vegetal cortical localization of Dsh and the putative, local activation of this protein in the vegetal region of the embryo.

We thank J. Miller and R. Moon for plasmids encoding Xl-wt-β-catenin-GFP and Xl-pt-β-catenin-GFP, D. Kimelman for plasmid encoding Xl-dnGSK3β, and D. McClay for antibody against Lv-β-catenin. C.A.E. was supported by grants from the NSF and NIH and A.W. was supported by grants from the NSF and the Hawaii Community Foundation.

References

Axelrod, J. D., Miller, R., Shulman, J. M., Moon, R. T. and Perrimon, N. (1998). Differential recruitment of Dishevelled provides signaling specificity in the planar cell polarity and Wingless signaling pathways. *Genes Dev.* **12**, 2610-2622.

Byers, S., Pishvaian, M., Crockett, C., Peer, C., Tozeren, A., Sporn, M., Anzano, M. and Lechleider, R. (1996). Retinoids increase cell-cell adhesion strength, beta-catenin protein stability, and localization to the cell membrane in a breast cancer cell line: a role for serine kinase activity. *Endocrinology* **137**, 3265-3273.

Capelluto, D. G., Kutateladze, T. G., Habas, R., Finkielstein, C. V., He, X. and Overduin, M. M. (2002). The DIX domain targets dishevelled to actin stress fibres and vesicular membranes. *Nature* **419**, 726-729.

Chan, S. K. and Struhl, G. (2002). Evidence that Armadillo transduces wingless by mediating nuclear export or cytosolic activation of Pangolin. *Cell* **111**, 265-280.

Davidson, E. H., Rast, J. P., Oliveri, P., Ransick, A., Calestani, C., Yuh, C. H., Minokawa, T., Amore, G., Hinman, V., Arenas-Mena, C. et al. (2002). A provisional regulatory gene network for specification of endomesoderm in the sea urchin embryo. *Dev. Biol.* **246**, 162-190.

Dominguez, I. and Green, J. B. (2000). Dorsal downregulation of GSK3β by a non-Wnt-like mechanisms is an early molecular consequence of cortical rotation in early Xenopus embryos. *Development* **127**, 861-868.

Emily-Fenouil, F., Ghiglione, C., Lhomond, G., Lepage, T. and Gache, C. (1998). GSK3β/shaggy mediates patterning along the animal-vegetal axis of the sea urchin embryo. *Development* **125**, 2489-2498.

Ettensohn, C. A, Illies, M. R., Oliveri, P. and De Jong, D. L. (2003). Alx1, a member of the Cart1/Alx3/Alx4 subfamily of Paired-class homeodomain proteins, is an essential component of the gene network controlling skeletogenic fate specification in the sea urchin embryo. *Development* **130**, 2917-2928.

Ferkey, D. M. and Kimelman, D. (2002). Glycogen synthase kinase-3 beta mutagenesis identifies a common binding domain for GBP and Axin. *J. Biol. Chem.* **277**, 16147-16152.

Fuchikami, T., Mitsunaga-Nakatsubo, K., Amemiya, S., Hosomi, T., Watanabe, T., Kurokawa, D., Kataoka, M., Harada, Y., Satoh, N., Kusunoki, S. et al. (2002). T-brain homologue (HpTb) is involved in the archenteron induction signals of micromere descendant cells in the sea urchin embryo. *Development* **129**, 5205-5216.

Guger, K. A. and Gumbiner, B. M. (2000). A mode of regulation of β-catenin signaling activity in Xenopus embryos independent of its levels. *Dev. Biol.* **223**, 441-448.

Heasman, J., Crawford, A., Goldstone, K., Garner-Hamrick, P., Gumbiner, B., McCrea, P., Kintner, C., Noro, C. Y. and Wylie, C. (1994). Overexpression of cadherins and underexpression of beta-catenin inhibit dorsal mesoderm induction in early Xenopus embryos. *Cell* **79**, 791-803.

Henderson, B. R. and Fagotto, F. (2002). The ins and outs of APC and beta-catenin nuclear transport. *EMBO J.* **3**, 834-839.

Hino, S., Michiue, T., Asashima, M. and Kikuchi, A. (2003). Casein kinase I epsilon enhances the binding of Dvl-1 to Frat-1 and is essential for Wnt-3a-induced accumulation of beta-catenin. *J. Biol. Chem.* **278**, 14066-14073.

Hsu, W., Zeng, L. and Costantini, F. (1999). Identification of a domain of Axin that binds to the serine/threonine protein phosphatase 2A and a self-binding domain. *J. Biol. Chem.* **274**, 3439-3445.

Huelsken, J. and Behrens, J. (2002). The Wnt signalling pathway. *J. Cell Sci.* **115**, 3977-3978.

Imai, K., Takada, N., Satoh, N. and Satou, Y. (2000). Beta-catenin mediates the specification of endoderm cells in ascidian embryos. *Development* **127**, 3009-3020.

Itoh, K., Antipova, A., Ratcliffe, M. J. and Sokol, S. (2000). Interaction of dishevelled and Xenopus Axin-related protein is required for wnt signal transduction. *Mol. Cell Biol.* **20**, 2228-2238.

Kelly, C., Chin, A. J., Leatherman, J. L., Kozlowski, D. J. and Weinberg, E. S. (2000). Maternally controlled β-catenin-mediated signaling is required for organizer formation in the zebrafish. *Development* **127**, 3899-3911.

Kelly, G. M., Erezyilmaz, D. F. and Moon, R. T. (1995). Induction of a secondary embryonic axis in zebrafish occurs following the overexpression of beta-catenin. *Mech. Dev.* **53**, 261-273.

Kishida, S., Yamamoto, H., Hino, S., Ikeda, S., Kishida, M. and Kikuchi, A. (1999). DIX domains of Dvl and axin are necessary for protein interactions and their ability to regulate beta-catenin stability. *Mol. Cell Biol.* **19**, 4414-4422.

Kurokawa, D., Kitajima, T., Mitsunaga-Nakatsubo, K., Amemiya, S., Shimada, H. and Akasaka, K. (1999). *Hp-ets*, an ets-related transcription factor implicated in primary mesenchyme cell differentiation in the sea urchin embryo. *Mech. Dev.* **80**, 41-52.

Larabell, C. A., Torres, M., Rowning, B. A., Yost, C., Miller, J. R., Wu, M., Kimelman, D. and Moon, R. T. (1997). Establishment of the dorso-ventral axis in Xenopus embryos is presaged by early asymmetries in β-catenin that are modulated by the Wnt signaling pathway. *J. Cell Biol.* **136**, 1123-1136.

Li, L., Yuan, H., Weaver, C. D., Mao, J., Farr, G. H. 3rd, Sussman, D. J., Jonkers, J., Kimelman, D. and Wu, D. (1999). Axin and Frat1 interact with dvl and GSK, bridging Dvl to GSK in Wnt-mediated regulation of LEF-1. *EMBO J.* **18**, 4233-4240.

Liu, C., Li, Y., Semenov, M., Han C., Baeg, G.-H., Tan, Y., Zhang, Z., Lin, X. and He, X. (2002). Control of beta-catenin phosphorylation/degradation by a dual-kinase mechanism. *Cell* **108**, 837-847.

Logan, C. Y., Miller, J. R., Ferkowicz, M. J. and McClay, D. R. (1999). Nuclear β-catenin is required to specify vegetal cell fates in the sea urchin embryo. *Development* **126**, 345-357.

McClay, D. R., Peterson, R. E., Range, R. C., Winter-Vann, A. M. and Ferkowicz, M. J. (2000). A micromere induction signal is activated by beta-catenin and acts through notch to initiate specification of secondary mesenchyme cells in the sea urchin embryo. *Development* **127**, 5113-5122.

Miller, J. R. and McClay, D. R. (1997). Changes in the pattern of adherens junction-associated beta-catenin accompany morphogenesis in the sea urchin embryo. *Dev. Biol.* **192**, 310-322.

Miller, J. R., Rowning, B. A., Larabell, C. A., Yang-Snyder, J. A., Bates, R. L. and Moon, R. T. (1999). Establishment of the dorsal-ventral axis in Xenopus embryos coincides with the dorsal enrichment of dishevelled that is dependent on cortical rotation. *J. Cell Biol.* **146**, 427-437.

Moon, R. T. and Kimelman, D. (1998). From cortical rotation to organizer gene expression: toward a molecular explanation of axis specification in Xenopus. *BioEssays* **20**, 536-545.

Moon, R. T., Bowerman, B., Boutros, M. and Perrimon, N. (2002). The promise and perils of Wnt signaling through beta-catenin. *Science* **296**, 1644-1646.

Oliveri, P., Carrick, D. M. and Davidson, E. H. (2002). A regulatory gene network that directs micromere specification in the sea urchin embryo. *Dev. Biol.* **246**, 209-228.

Oliveri, P., Davidson, E. H. and McClay, D. R. (2003). Activation of pmar1 controls specification of micromeres in the sea urchin embryo. *Dev. Biol.* **258**, 32-43.

Pai, L. M., Orsulic, S., Bejsovec, A. and Peifer, M. (1997). Negative regulation of Armadillo, a Wingless effector in *Drosophila*. *Development* **124**, 2255-2266.

Pelegri, F. and Maischein, H. M. (1998). Function of zebrafish beta-catenin and TCF-3 in dorsoventral patterning. *Mech. Dev.* **77**, 63-74.

Penton, A., Wodarz, A. and Nusse, R. A. (2002). A mutational analysis of dishevelled in Drosophila defines novel domains in the dishevelled protein as well as novel suppressing alleles of axin. *Genetics* **161**, 747-762.

Roeser, T., Stein, S. and Kessel, M. (1999). Nuclear beta-catenin and the development of bilateral symmetry in normal and LiCl-exposed chick embryos. *Development* **126**, 2955-2966.

Rothbacher, U., Laurent, M. N., Deardorff, M. A., Klein, P. S., Cho, K. W. and Fraser, S. E. (2000). Dishevelled phosphorylation, subcellular localization and multimerization regulate its role in early embryogenesis. *EMBO J.* **19**, 1010-1022.

Rowning, B. A., Wells, J., Wu, M., Gerhart, J. C., Moon, R. T. and Larabell, C. A. (1997). Microtubule-mediated transport of organelles and localization of beta-catenin to the future dorsal side of Xenopus eggs. *Proc. Natl. Acad. Sci. USA* **94**, 1224-1229.

Sakanaka, C. and Williams, L. T. (1999). Functional domains of axin. Importance of the C terminus as an oligomerization domain. *J. Biol. Chem.* **274**, 14090-14093.

Schneider, S., Steinbeisser, H., Warga, R. M. and Hausen, P. (1996). Beta-catenin translocation into nuclei demarcates the dorsalizing centers in frog and fish embryos. *Mech. Dev.* **57**, 191-198.

Sokol, S. Y. (1996). Analysis of Dishevelled signalling pathways during Xenopus development. *Curr. Biol.* **6**, 1456-1467.

Sokol, S. (1999). Wnt signaling and dorso-ventral axis specification in vertebrates. *Curr. Opin. Gen. Dev.* **9**, 405-410.

Sun, T. Q., Lu, B., Feng, J. J., Reinhard, C., Jan, Y. N., Fantl, W. J. and Williams, L. T. (2001). PAR-1 is a Dishevelled-associated kinase and a positive regulator of Wnt signalling. *Nat. Cell Biol.* **3**, 628-636.

Sweet, H. C., Gehring, M. and Ettensohn, C. A. (2002). LvDelta is a mesoderm-inducing signal in the sea urchin embryo and can endow blastomeres with organizer-like properties. *Development* **129**, 1945-1955.

Tolwinski, N. S., Wehrli, M., Rives, A., Erdeniz, N., DiNardo, S. and Wieschaus, E. (2003). Wg/Wnt signal can be transmitted through arrow/LRP5,6 and Axin independently of Zw3/Gsk3beta activity. *Dev. Cell* **4**, 407-418.

Vonica, A., Weng, W., Gumbiner, B. M. and Venuti, J. M. (2000). TCF is the nuclear effector of the beta-catenin signal that patterns the sea urchin animal-vegetal axis. *Dev. Biol.* **217**, 230-243.

Wharton, K. A. (2003). Runnin' with the Dvl: proteins that associate with Dsh/Dvl and their significance to Wnt signal transduction. *Dev. Biol.* **253**, 1-17.

Wikramanayake, A. H., Hong, M., Lee, P. N., Pang, K., Byrum, C. A., Bince, J. M., Xu, R. and Martindale, M. Q. (2003). An ancient role for nuclear beta-catenin in the evolution of axial polarity and germ layer segregation. *Nature* **426**, 446-450.

Wikramanayake, A. H., Huang, L. and Klein, W. H. (1998). Beta-catenin is essential for patterning the maternally specified animal-vegetal axis in the sea urchin embryo. *Proc. Natl. Acad. Sci. USA* **95**, 9343-9348.

Wylie, C., Kofron, M., Payne, C., Anderson, R., Hosobuchi, M., Joseph, E. and Heasman, J. (1996). Maternal beta-catenin establishes a 'dorsal signal' in early Xenopus embryos. *Development* **122**, 2987-2996.

Yost, C., Torres, M., Miller, J. R., Huang, E., Kimelman, D. and Moon, R. T. (1996). The axis-inducing activity, stability, and subcellular distribution of β-catenin is regulated in Xenopus embryos by glycogen synthase kinase 3. *Genes Dev.* **10**, 1443-1454.

Zhu, X., Mahairas, G., Illies, M., Cameron, R. A., Davidson, E. H. and Ettensohn, C. A. (2001). A large-scale analysis of mRNAs expressed by primary mesenchyme cells of the sea urchin embryo. *Development* **128**, 2615-2627.